

HeteroRAG: A Heterogeneous Retrieval-Augmented Generation Framework for Medical Vision Language Tasks

Zhe Chen^{1,3}, Yusheng Liao^{1,3}, Shuyang Jiang^{2,3}, Zhiyuan Zhu¹, Haolin Li^{2,3}
Yanfeng Wang^{1,3}, Yu Wang^{1,3*}

¹Shanghai Jiao Tong University ²Fudan University ³Shanghai Artificial Intelligence Laboratory
{chenzhe2018, yuwangsju}@sjtu.edu.cn

Abstract

Medical large vision-language Models (Med-LVLMs) have shown promise in clinical applications but suffer from factual inaccuracies and unreliable outputs, posing risks in real-world diagnostics. While retrieval-augmented generation has emerged as a potential solution, current medical multimodal RAG systems are unable to perform effective retrieval across heterogeneous sources. The irrelevance of retrieved reports affects the factuality of analysis, while insufficient knowledge affects the credibility of clinical decision-making. To bridge the gap, we construct MedAtlas, which includes extensive multimodal report repositories and diverse text corpora. Based on it, we present HeteroRAG, a novel framework that enhances Med-LVLMs through heterogeneous knowledge sources. The framework introduces Modality-specific CLIPs for effective report retrieval and a Multi-corpora Query Generator for dynamically constructing queries for diverse corpora. Incorporating knowledge from such multifaceted sources, Med-LVLM is then trained with Heterogeneous Knowledge Preference Tuning to achieve cross-modality and multi-source knowledge alignment. Extensive experiments across 12 datasets and 3 modalities demonstrate that the proposed HeteroRAG achieves state-of-the-art performance in most medical vision language benchmarks, significantly improving factual accuracy and reliability of Med-LVLMs.

1 Introduction

Large vision-language models (LVLMs) have made significant strides in integrating multimodal information and generating natural responses (Chen et al. 2024b; Comanici et al. 2025; Bai et al. 2025). Similarly, medical LVLMs (Med-LVLMs) show increasing promise for multimodal diagnosis and clinical decision support (Chen et al. 2024a; Lin et al. 2025; Xu et al. 2025). However, despite these advances, current Med-LVLMs still struggle with critical challenges related to factual accuracy and reliability (Sun et al. 2025; Xia et al. 2025). This limitation poses serious risks in medical applications, where errors could lead to misdiagnosis or harmful treatment recommendations.

To mitigate these limitations, recent scholarly efforts have prioritized multimodal retrieval-augmented generation (MMRAG) frameworks, which augment Med-LVLMs with medical knowledge to enhance diagnostic accuracy and

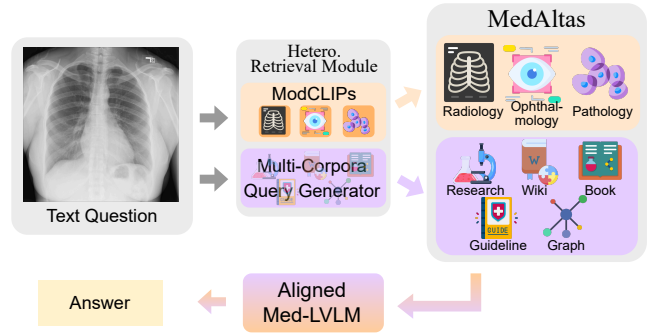


Figure 1: Overview of HeteroRAG Framework. The HRM retrieves reports and documents from MedAtlas for a knowledge-aligned Med-LVLM.

epistemic reliability (Ranjit et al. 2023; Sun et al. 2025; Choi et al. 2025; Shaaban et al. 2025). Predominant methodologies employ multimodal retrievers, such as the medical modality-aware CLIP models, to retrieve relevant reports using input images, owing to the strong semantic similarity between medical imaging and textual reports (Sun et al. 2025; Xia et al. 2024, 2025). However, the training data used to enhance the modality awareness of these retrievers is typically limited to the training splits of only a few datasets. This constraint leads to inferior retrieval performance and irrelevant retrieved reports, undermining the factuality of the Med-LVLMs. Moreover, medical corpora, such as research articles, textbooks, and clinical guidelines, are crucial for enhancing the reliability of Med-LVLMs. However, the multimodal retrievers fail when applied to them, as they lack direct visual semantics and exhibit diverse linguistic characteristics. Current efforts (Wu et al. 2025; Hamza et al. 2025) attempt cross-modality document retrieval using the original multimodal query. Though straightforward, they neglect the alignment between queries and corpus characteristics. One concurrent work, MIRA (Wang et al. 2025), which employs LLM-rewritten queries for improved clarity, still fails in tailored retrieval due to limited information presented in the rewriting prompt. In summary, current approaches fail to perform effective retrieval across heterogeneous sources, resulting in a significant knowledge gap and undermining the factuality and credibility of medical MMRAG systems.

*Corresponding author.

A key bottleneck in addressing these limitations is the lack of a diverse and sufficient knowledge base. To fill the gap, we construct **MedAtlas**, which comprises broad multimodal report repositories and rich text corpora. The report repositories contain image-text reports in radiology, ophthalmology, and pathology. The text corpora are compiled from research articles, Wikipedia entries, medical textbooks, clinical guidelines, and knowledge graphs.

Building upon MedAtlas, we propose HeteroRAG, a framework designed to significantly enhance the factual accuracy and reliability of Med-LVLMs. As illustrated in Figure 1, we develop the Heterogeneous Retrieval Module (HRM), which integrates Modality-specific CLIPs (Mod-CLIPs) and a Multi-corpora Query Generator (MQG). Mod-CLIPs are trained on large-scale data to ensure effective cross-modality report retrieval. The MQG module is trained in two stages to capture corpus-specific characteristics and generate tailored queries. Finally, we propose the Heterogeneous Knowledge Preference Tuning (HKPT) method to achieve two types of alignment: (1) cross-modality alignment, which aligns visual inputs with retrieved textual content; and (2) multi-source knowledge alignment, which aligns the model’s internal knowledge with external knowledge from diverse sources.

We evaluate HeteroRAG on medical visual question answering and report generation tasks across 3 modalities and 12 datasets. Empirical results show that our framework achieves state-of-the-art performances on most benchmarks, demonstrating its strong factuality and reliability. Notably, HeteroRAG surpasses public Med-LVLMs, which contain 4–5× parameters, highlighting the value of effective knowledge integration and alignment.

Our contributions are summarized as follows:

- We introduce MedAtlas, a newly curated comprehensive medical database that provides rich multimodal knowledge for Med-LVLMs and establishes a robust foundation for medical MMRAG research.
- Leveraging MedAtlas, we propose HeteroRAG, a novel medical MMRAG framework that performs accurate heterogeneous knowledge retrieval and fine-grained knowledge alignment.
- Extensive experiments validate HeteroRAG’s capability to precisely retrieve and effectively integrate multi-source knowledge, demonstrating SOTA performance across most benchmarks. The framework also consistently outperforms substantially larger Med-LVLMs and establishes a trustworthy and reliable foundation for medical knowledge-intensive applications.

2 Related Work

Medical Report Retrieval for Generation. Existing Medical MMRAG approaches primarily utilize the medical images to retrieve relevant reports (He et al. 2024; Sun et al. 2025; Xia et al. 2024, 2025). For instance, FactMM-RAG (Sun et al. 2025) enhances report generation by incorporating high-quality reference reports. Similarly, RULE (Xia et al. 2024) and MMed-RAG (Xia et al. 2025) integrate reference reports and employ preference

fine-tuning to improve model utilization of retrieved reports. Although these approaches improve the factual accuracy of responses, they neglect the retrieval of medical documents, which are crucial for Med-LVLM’s reliable inference.

Medical Document Retrieval for Generation. Acknowledging the limitations of report-only retrieval, recent studies have increasingly emphasized medical documents as knowledge sources (Choi et al. 2025; Shaaban et al. 2025; Wu et al. 2025; Hamza et al. 2025). Among them, MKGF (Wu et al. 2025) and K-LLaVA (Hamza et al. 2025) both employ multimodal retrievers to fetch documents from the database, aiming to mitigate hallucination issues in language models. ChatCAD+ (Zhao et al. 2024b) and MIRA (Wang et al. 2025) utilize a zero-shot query rewriting module for retrieval. Nevertheless, these retrieval methods overlook the substantial content differences among various corpora, lacking corpus-specific retrieval mechanisms.

3 MedAtlas Knowledge Base

The MedAtlas knowledge base comprises comprehensive multimodal report repositories covering three modalities and rich textual corpora from five distinct sources.

3.1 Multimodal Report Repository

Existing medical image-report repositories are limited in scale and diversity. To address this issue, we collect image-report pairs from a wide range of datasets. Specifically, the Radiology subset includes 1,104,313 pairs from 6 datasets; the Ophthalmology subset includes 111,991 pairs from 5 datasets; and the Pathology subset includes 1,514,058 pairs from 5 datasets. To ensure data quality, duplicate pairs are removed using the image perceptual hashing algorithm (Du, Ho, and Cong 2020). More details are provided in Appendix B.1. For the retrieval method, we use images as queries and reports in the library as keys to retrieve the top-k reports, following Sun et al. (2025); Xia et al. (2024, 2025).

3.2 Textual Corpora

To ensure the richness, we collect corpora from five representative sources. The **Research** corpus is drawn from the 2025 PubMed Annual Baseline. The **Wiki** corpus is collected from the Wikipedia dumps. The **Book** corpus contains e-books from PMC-LLaMA (Wu et al. 2024a), MedQA Textbook, and StatPearls, providing foundational medical knowledge (Xiong et al. 2024; Fan, Wang, and Liu 2025; Chen et al. 2025). The **Guideline** corpus contains clinical guidelines crawled from authoritative websites following Chen et al. (2023). For the above four corpora, they are chunked into chunks of no more than 1000 characters, with an overlap of 200 characters following Xiong et al. (2024). The **Graph** corpus is collected from UMLS. Finally, the Research, Wiki, Book, and Guideline corpora contain 51.2M, 29.7M, 14.1M, and 657.9K chunks, respectively. The Graph corpus includes 1.7M terms and 2.9M relations.

For the retrieval of unstructured corpora, each query is formatted as “query”, and the MedCPT models (Jin et al. 2023) are used for vector search and reranking. For the structured Graph corpus, each query is formatted as “query.term,

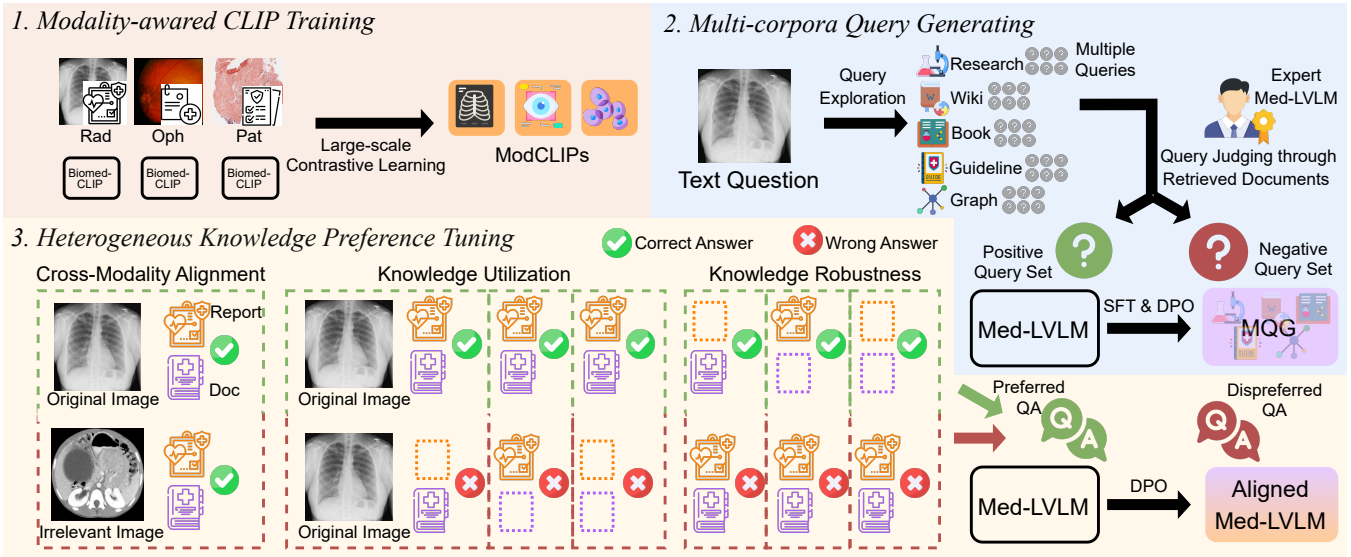


Figure 2: Overview of HeteroRAG framework. It introduces the Modality-specific CLIPs for effective report retrieval. Then, the Multi-corpora Query Generator is developed for tailored retrieval for different corpora. Finally, HKPT is conducted to achieve the cross-modality and multi-source knowledge alignment.

query_relation”. Given the “query_term”, its definition and one-hop relationships are retrieved, followed by filtering relevant relationships by reranking with “query_relation” (Yang et al. 2024).

4 HeteroRAG Framework

In this section, we present the HeteroRAG framework, as illustrated in Figure 2. First, we introduce Modality-specific CLIPs (ModCLIPs), which are trained on large-scale image-text pairs for accurate report retrieval. Next, a Multi-corpora Query Generator (MQG) is developed to enable tailored retrieval for multimodal questions based on corpus characteristics. Finally, we propose a Heterogeneous Knowledge Preference Tuning (HKPT) method to realize cross-modality and multi-source knowledge alignment.

4.1 Modality-specific CLIPs

The ModCLIPs are initialized from BiomedCLIP (Zhang et al. 2023). For each modality, the report retrieval base is independently split into training, development, and test sets to fine-tune CLIP models, following Xia et al. (2024, 2025). Specifically, all samples of each modality are randomly split into 2000 development samples, 2000 test samples, and the remainder for training. This results in 1.10M image-text training pairs in radiology, 0.11M in ophthalmology, and 1.51M in pathology. Contrastive learning (Radford et al. 2021) is performed on single-modality image-text pairs for each ModCLIP. Compared to previous work (Sun et al. 2025; Xia et al. 2024, 2025), which relied solely on training splits from a limited number of datasets, the significantly scaled-up training data enables more accurate cross-modal report retrieval.

4.2 Multi-corpora Query Generator

For each multimodal question including the image v and text question t , the module generates query set for each corpus $Q = \{(i, j, q_j^i) \mid i = 1, 2, \dots, N_C, j = 1, 2, \dots, N_q^i\}$, where q_j^i denotes the j_{th} query for the i_{th} corpus, N_C denotes the number of corpora, and N_q^i denotes the number of queries for the i_{th} corpus. Each query is then used to retrieve documents that collectively support answering (v, t) . The training pipeline for MQG is as follows.

We begin with a query exploration phase to identify potential retrieval strategies. Since annotations for documents supporting medical multimodal questions are generally unavailable, we use the expert Med-LVLM, Lingshu-32B (Xu et al. 2025) to generate proxy labels, as inspired by Chen et al. (2025). Lingshu-32B consistently achieves SOTA performances across most medical vision language tasks. We prompt the expert Med-LVLM to generate multiple queries for each source. The prompts are designed to encourage intra-corpus diversity and align with the characteristics of corpora. To control the cost, the number of exploration queries per corpus is fixed to 6. Subsequently, the same expert model evaluates the documents retrieved by each query by judging whether they support the reference answer. Manual evaluation of judgment quality is conducted on a 300-item subset by medical researchers. The results show that Lingshu-32B achieves an accuracy of 0.837 and an F1 score of 0.870, demonstrating the reliability of VLM-as-a-judge. Based on the judgment, queries are categorized as either positive, denoted q_w , or negative, denoted q_l .

For each corpus, we select up to N_q^i instances of q_w and q_l to form positive queries Q_w and negative queries Q_l , respectively. A two-stage training strategy is applied to MQG. First, supervised fine-tuning (SFT) is performed:

Algorithm 1: Heterogeneous Knowledge Preference Tuning (HKPT)

Input: $\mathcal{D} = \{v^i, t^i, K^i, y^i\}_{i=1}^N$: Training dataset;
 $K = \{k_r, k_d\}$: Retrieved knowledge; \mathcal{M}_θ :
Med-LVLM; $\mathcal{D}_{cm}, \mathcal{D}_{mk}$: Preference datasets.

Output: \mathcal{M} : Preference tuned model.

```
1 Initialize  $\mathcal{D}_{cm}, \mathcal{D}_{mk}$  with empty sets
2 foreach  $(v, t, K, y) \in \mathcal{D}$  do
3   Retrieve the image  $v^*$  irrelevant to  $v$ 
4    $\triangleright$  Cross-Modality Alignment
5   if  $\mathcal{M}(v, t, K) = y$  and  $\mathcal{M}(v^*, t, K) = y$  then
6      $x_w \leftarrow (v, t, K)$ ;  $y_w \leftarrow y$ 
7      $x_l \leftarrow (v^*, t, K)$ ;  $y_l \leftarrow \mathcal{M}(v^*, t, K)$ 
8     Put  $\{x_w, x_l, y_w, y_l\}$  into  $\mathcal{D}_{cm}$ 
9    $\triangleright$  Multi-Source Knowledge Alignment
10  foreach  $k \in \{\{k_r\}, \{k_d\}, \{k_r, k_d\}\}$  do
11     $\triangleright$  Knowledge Utilization
12    if  $\mathcal{M}(v, t, K) = y$  and  $\mathcal{M}(v, t, K \setminus k) \neq y$  then
13       $x_w \leftarrow (v, t, K)$ ;  $y_w \leftarrow y$ 
14       $x_l \leftarrow (v, t, K)$ ;  $y_l \leftarrow \mathcal{M}(v, t, K \setminus k)$ 
15      Put  $\{x_w, x_l, y_w, y_l\}$  into  $\mathcal{D}_{mk}$ 
16     $\triangleright$  Knowledge Robustness
17    if  $\mathcal{M}(v, t, K \setminus k) = y$  and  $\mathcal{M}(v, t, K) \neq y$  then
18       $x_w \leftarrow (v, t, K)$ ;  $y_w \leftarrow y$ 
19       $x_l \leftarrow (v, t, K)$ ;  $y_l \leftarrow \mathcal{M}(v, t, K)$ 
20      Put  $\{x_w, x_l, y_w, y_l\}$  into  $\mathcal{D}_{mk}$ 
21 foreach  $(x_w, x_l, y_w, y_l) \in \mathcal{D}_{cm} \cup \mathcal{D}_{mk}$  do
22   Compute the loss and update  $\mathcal{M}$  following Eq. 3
```

$$\mathcal{L}_{\text{SFT}} = -\mathbb{E}_{(v,t,Q_w) \sim \mathcal{D}_w} \log \mathcal{M}_\theta(Q_w | v, t). \quad (1)$$

Then, direct preference optimization (DPO) is applied to further align the retrieval strategies with corpora:

$$\mathcal{L}_{\text{DPO}}(\mathcal{M}_\theta; \mathcal{M}_{\text{ref}}) = -\mathbb{E}_{(v,t,Q_w,Q_l) \sim \mathcal{D}_{wl}} \left[\log \sigma \left(\beta \log \frac{\mathcal{M}_\theta(Q_w|v,t)}{\mathcal{M}_{\text{ref}}(Q_w|v,t)} - \beta \log \frac{\mathcal{M}_\theta(Q_l|v,t)}{\mathcal{M}_{\text{ref}}(Q_l|v,t)} \right) \right]. \quad (2)$$

4.3 Heterogeneous Knowledge Preference Tuning

Despite retrieving relevant reports and reliable documents, Med-LVLMs still suffer from severe knowledge misalignment issues. Inspired by RULE (Xia et al. 2024) and MMed-RAG (Xia et al. 2025), which introduce the preference fine-tuning strategy for aligning Med-LVLMs with external reports, we propose Heterogeneous Knowledge Preference Tuning (HKPT) to enable alignment with knowledge from more sources. The HKPT process is detailed in Algorithm 1.

Cross-Modality Alignment. The incorporation of external knowledge may cause Med-LVLM to ignore visual information and directly copy retrieved contents (Xia et al. 2025). To mitigate this, we construct preference pairs from the training set to improve modality alignment. Each training sample is denoted as $\{v, t, K, y\}$, where v is the medical image, t is the text question, K is the retrieved knowledge (including reports k_r and documents k_d), and y is the gold answer. For each v , we retrieve the least similar image from the same modality training samples as an irrelevant image v^* . Preferred responses are selected when \mathcal{M} correctly

answers using v , while dispreferred ones are selected when \mathcal{M} correctly answers using irrelevant v^* , indicating that \mathcal{M} ignores v and relies solely on K . For open-ended generation tasks, correctness is defined as the average metric exceeding a threshold α_r . The criterion also applies below. This process forms the preference dataset \mathcal{D}_{cm} .

Multi-Source Knowledge Alignment. To improve \mathcal{M} 's alignment with external knowledge K , which includes reports k_r and documents k_d , we design preference pairs from two aspects: **knowledge utilization and robustness**. Taking k_r as an example: For knowledge utilization, preferred responses are selected when \mathcal{M} correctly answers by properly using k_r , while dispreferred ones are selected when \mathcal{M} fails without k_r . For knowledge robustness, preferred responses are selected when \mathcal{M} correctly answers without k_r , while dispreferred ones are selected when \mathcal{M} misuses k_r and produces incorrect answers. The dual-aspect strategy is also applied to k_d , and a combination of k_r and k_d , ensuring fine-grained alignment across all knowledge sources.

The resulting \mathcal{D}_{mk} , together with \mathcal{D}_{cm} , are employed in HKPT, enabling unified alignment across modalities and knowledge sources:

$$\mathcal{L}_{\text{HKPT}}(\mathcal{M}_{\theta'}; \mathcal{M}_{\text{ref}'}) = -\mathbb{E}_{(x_w, x_l, y_w, y_l) \sim \mathcal{D}_{cm} \cup \mathcal{D}_{mk}} \left[\log \sigma \left(\beta \log \frac{\mathcal{M}_{\theta'}(y_w|x_w)}{\mathcal{M}_{\text{ref}'}(y_w|x_w)} - \beta \log \frac{\mathcal{M}_{\theta'}(y_l|x_l)}{\mathcal{M}_{\text{ref}'}(y_l|x_l)} \right) \right]. \quad (3)$$

5 Experiments

5.1 Experimental Setups

Datasets and Metrics. The medical VQA datasets include OMVQA-Rad (Hu et al. 2024), VQA-RAD (Lau et al. 2018), SLAKE (Liu et al. 2021), OMVQA-Oph (Hu et al. 2024), DME-VQA (Tascon-Morales, Márquez-Neila, and Sznitman 2022), Quilt-VQA (Seyfioglu et al. 2024), PathMMU (Sun et al. 2024a), and PathVQA (He et al. 2020). Medical report generation datasets include MIMIC-CXR (Johnson et al. 2019), IU-Xray (Demner-Fushman et al. 2015), Harvard-FairVLMed (Luo et al. 2024), and DeepEyeNet (Huang et al. 2021). We have carefully checked and ensured that no sample overlap exists between these datasets and the report database. **This guarantees that the dataset samples are unseen during ModCLIPs' training and prevents the retrieval results from containing instances identical to the samples. Note that the performance on Quilt-VQA can be seen as out-of-distribution results, as the dataset does not include a training split.** Additional dataset details are provided in Appendix B.2.

For evaluation metrics, accuracy is used for closed-ended medical VQA tasks. Radiology report generation is evaluated using BLEU (Papineni et al. 2002), ROUGE-L (Lin 2004), and RaTEScore (Zhao et al. 2024a), while ophthalmology report generation is evaluated using BLEU, ROUGE-L, and METEOR¹ (Banerjee and Lavie 2005).

Implementation Details. For the SFT and DPO training of the MQG, we employ LoRA (Hu et al. 2022) to train the

¹RaTEScore is not used for evaluating ophthalmology report generation, as it is specifically for radiology.

Methods	Retrieval	Radiology			Ophthalmology		Pathology		
		OMVQA-Rad	VQA-RAD	SLAKE	OMVQA-Oph	DME-VQA	Quilt-VQA	PathMMU	PathVQA
Original	-	74.92	72.79	83.65	80.83	81.92	49.27	57.36	77.38
Beam Search	-	74.25	72.43	84.86	80.58	81.92	48.40	55.85	75.97
DoLa	-	74.33	73.16	84.86	80.75	81.54	50.44	55.69	77.03
VCD	-	74.42	72.06	83.17	80.83	81.62	45.48	54.68	76.50
AVISC	-	70.33	74.63	83.65	80.25	81.08	53.94	56.52	79.50
M3ID	-	72.50	74.63	81.97	82.58	82.61	49.27	53.34	77.38
MedDr	Report	78.33	74.26	83.65	83.75	81.24	53.06	62.21	77.74
FactMM-RAG	Report	79.00	76.10	85.58	85.67	85.74	58.60	65.55	86.64
RULE	Report	76.17	75.00	83.17	83.67	82.84	61.22	66.56	84.13
MMed-RAG	Report	<u>79.50</u>	<u>78.31</u>	87.26	<u>88.17</u>	86.73	<u>67.06</u>	<u>71.74</u>	87.56
MKGF	Doc	74.25	74.63	84.86	82.33	82.07	58.02	66.22	80.06
K-LLaVA	Doc	75.83	75.00	86.30	85.25	83.22	61.81	69.23	84.02
MIAR	Report+Doc	78.67	75.74	85.82	87.92	83.14	65.01	72.07	88.62
HeteroRAG (Ours)	Report+Doc	82.08	80.51	<u>86.78</u>	91.25	83.68	69.97	75.08	91.45

Table 1: Model performance of different methods based on Lingshu-7B on the medical VQA task. The best results and second-best results are highlighted in **bold** and underlined, respectively.

model initialized from Lingshu-7B. The HKPT process is also conducted using LoRA based on Lingshu-7B. For report retrieval, we adopt the adaptive retrieval context selection method (Xia et al. 2025). For document retrieval, the MQG generates up to four queries in total for unstructured corpora (all except Graph). Each query retrieves the top-10 documents, which are then reranked to select the top-2 documents. For the Graph corpus, the MQG retrieves one term and its reranked top-10 relations. The generation temperature is set to 0 to ensure reproducibility. More implementation details and detailed prompts are provided in Appendix B.4 and Appendix C, respectively.

Baselines. Four categories of baselines are introduced: (1) decoding-based methods aiming for improving factuality including Beam Search (Sutskever, Vinyals, and Le 2014), DoLa (Chuang et al. 2024), VCD (Leng et al. 2024), AVISC (Woo et al. 2024), and M3ID (Favero et al. 2024); (2) report-retrieval methods including MedDr (He et al. 2024), FactMM-RAG (Sun et al. 2025), RULE (Xia et al. 2024), and MMed-RAG (Xia et al. 2025); (3) document-retrieval methods including MKGF (Wu et al. 2025) and K-LLaMA (Hamza et al. 2025) and (4) a concurrent work that retrieves both reports and documents, MIRA (Wang et al. 2025). **To ensure fair comparison, retrievable reports and documents remain consistent across all baselines. Medical CLIPs for report retrieval also remain consistent across all baselines, with the impact of CLIP training data analyzed separately in Section 5.3.** We also introduce widely-used Med-LVLMs: LLaVA-Med-7B (Li et al. 2023), MedGemma-4B (Sjellergren et al. 2025), HuatuoGPT-V-34B (Chen et al. 2024a), HealthGPT-32B (Lin et al. 2025), and Lingshu-32B (Xu et al. 2025). More baseline details are shown in Appendix B.3.

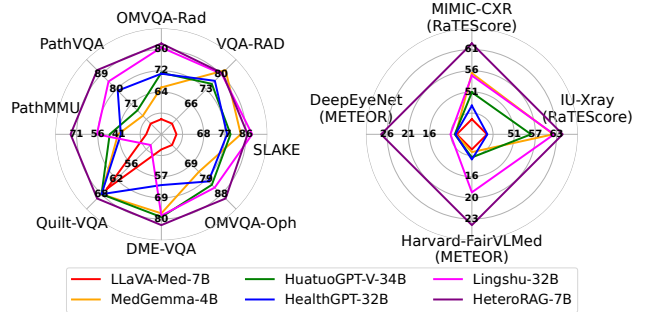


Figure 3: Comparison of HeteroRAG with other Med-LVLMs. Effective retrieval and fine-grained integration of external knowledge enables the HeteroRAG to surpass larger Med-LVLMs with greater parameter efficiency.

5.2 Main Results

The experimental results of different methods based on Lingshu-7B are presented in Table 1 and Table 2. A comparison between widely used Med-LVLMs and HeteroRAG is illustrated in Figure 3. These results lead to the following key observations: **(1) Effectiveness of incorporating multi-source knowledge:** HeteroRAG achieves superior performance compared to approaches under different retrieval settings. This demonstrates our effectiveness in retrieving and integrating heterogeneous knowledge. Highly relevant reports enhance the factual accuracy of Med-LVLMs, while evidence documents improve their reliability. **(2) Generalizability of our framework:** HeteroRAG achieves the best performance on nearly all datasets across three modalities. Notably, this superiority holds not only for closed-ended VQA tasks but also for open-ended report generation, which requires more sophisticated multimodal understanding and generation capabilities. **(3) Superiority over larger**

Methods	Retrieval	Radiology						Ophthalmology					
		MIMIC-CXR			IU-Xray			Harvard-FairVLMed			DeepEyeNet		
		BLEU	R-L	RaTE	BLEU	R-L	RaTE	BLEU	R-L	METEOR	BLEU	R-L	METEOR
Original	-	10.31	30.39	53.30	18.50	41.00	57.95	4.21	14.30	15.75	2.35	5.06	10.20
Beam Search	-	10.52	30.08	49.91	19.70	41.81	61.29	2.66	11.36	13.40	2.00	5.29	10.34
DoLa	-	10.62	30.84	53.33	18.84	40.97	59.06	5.02	15.75	18.56	2.34	5.13	10.06
VCD	-	11.96	27.05	49.21	19.81	35.20	56.33	7.02	11.51	14.32	2.64	4.28	9.32
AVISC	-	13.52	27.43	49.01	18.86	34.80	58.75	6.94	12.59	15.80	2.52	5.90	9.14
M3ID	-	11.00	28.95	51.42	17.09	35.53	56.41	7.22	13.94	16.84	2.57	6.06	9.52
MedDr	Report	16.77	34.11	56.61	22.37	40.86	62.20	8.19	21.40	22.98	3.64	5.16	11.54
FactMM-RAG	Report	16.82	36.22	57.20	21.82	42.69	63.22	9.15	22.56	20.76	14.91	22.22	<u>27.08</u>
RULE	Report	17.65	34.55	56.56	19.01	38.21	59.90	8.42	21.09	16.68	14.12	20.20	25.61
MMed-RAG	Report	17.65	34.84	55.72	22.40	38.96	62.67	9.89	23.27	22.10	14.36	21.36	26.36
MKGF	Doc	11.56	32.33	53.66	19.97	41.32	59.64	5.87	16.18	16.83	3.44	6.65	11.55
K-LLaVA	Doc	16.56	<u>37.88</u>	57.98	<u>23.41</u>	<u>43.74</u>	<u>64.07</u>	10.53	22.97	19.23	<u>14.89</u>	23.55	26.96
MIAR	Report+Doc	<u>17.89</u>	37.38	<u>58.90</u>	22.37	42.66	63.80	<u>10.99</u>	<u>23.42</u>	22.78	14.73	<u>23.46</u>	26.85
HeteroRAG (Ours)	Report+Doc	21.46	39.94	62.80	26.55	45.13	65.14	15.65	26.02	24.24	13.28	22.75	28.02

Table 2: Model performance of different methods based on Lingshu-7B on the medical report generation task. The best results and second-best results are highlighted in **bold** and underlined, respectively.

Methods	OMVQA-Rad	OMVQA-Oph	Quilt-VQA
Original	74.92	80.83	49.27
SFT	78.00	87.17	62.39
HeteroRAG	82.08	91.25	69.97
w/o Reports	79.17	88.92	59.77
w/o Doc	78.25	86.17	57.43
w/o Research	80.25	87.42	64.14
w/o Wiki	80.25	90.17	67.64
w/o Book	79.42	84.08	64.43
w/o Guideline	77.00	90.17	66.47
w/o Graph	81.58	88.67	69.68

Table 3: Performance of HeteroRAG after dropping each source of knowledge.

Med-LVLMs: Figure 3 shows that HeteroRAG, with a 7B parameter size, outperforms most advanced Med-LVLMs, which contain 4 to 5 times more parameters across multiple datasets. This indicates that the proposed framework advances the medical multimodal capabilities of existing Med-LVLMs to a higher level.

5.3 Effectiveness of Retrieved Knowledge

We conduct ablation studies to evaluate the contribution of knowledge sources as shown in Table 3. The ‘‘Original’’ and ‘‘SFT’’ settings represent the performance of the original Lingshu-7B and Lingshu-7B after SFT on the original training set, which does not include reports and documents. The other configurations examine HeteroRAG’s performance when either reports or documents are removed. The results show that retrieved knowledge significantly improves Med-LVLM’s performance compared to the Original baseline. The performance improvements from super-

Models	Rad.	Oph.	Pat.
BiomedCLIP	30.20	13.45	28.85
PMC-CLIP	30.05	19.80	23.35
PubMedCLIP*	13.35	-	-
MM-Retinal*	-	4.65	-
QuiltNet*	-	-	39.65
FactMM-RAG*	44.25	-	-
RULE*	31.80	18.90	-
MMed-RAG*	31.80	18.90	30.20
ModCLIPs*	79.40	47.55	77.35

Table 4: Image-to-text recall@5 of different retrievers. The asterisks (*) denote the modality-specific retrievers.

vised fine-tuning alone are insufficient to compensate for the absence of knowledge. When reports or documents are excluded, the performance degradation confirms that both sources are important for HeteroRAG’s knowledge-intensive inference. Furthermore, all five corpora contribute to Med-LVLM’s capacity.

5.4 Effectiveness of ModCLIPs

We evaluate ModCLIPs against other medical retrievers on image-to-text report retrieval tasks, as shown in Table 4. Generalist retrievers include BiomedCLIP and PMC-CLIP (Lin et al. 2023). Modality-specific retrievers include PubMedCLIP (Eslami, Meinel, and De Melo 2023), MM-Retinal (Wu et al. 2024b), QuiltNet (Ikezogwo et al. 2023), FactMM-RAG, RULE and MMed-RAG. Using the test set described in Section 4.1 with recall@5 as our evaluation metric, our experiments demonstrate that ModCLIPs consistently outperform competing methods across all three modalities. This superior performance can be attributed to

Methods	OMVQA-Rad	OMVQA-Oph	Quilt-VQA
CLIP	76.83	84.42	63.85
MQG	82.08	91.25	69.97
w/o DPO	81.08	88.17	65.60
w/o SFT	78.75	86.00	64.14

Table 5: Performance of HeteroRAG under two ablation settings: replacing MQG with CLIP-based retrieval, and removing the training stages of MQG.

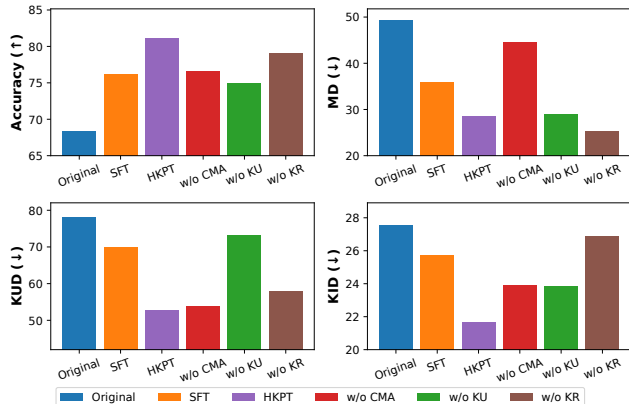


Figure 4: Accuracy and disalignment metrics of Lingshu-7B trained with different methods and data.

two key advantages: (1) Single-modality training yields significantly better modality-specific understanding compared to mixed-modality approaches, and (2) our training data offers more comprehensive coverage and greater diversity within each modality.

5.5 Effectiveness of MQG

We further investigate the effectiveness of MQG in Table 5. First, the MQG in HeteroRAG is replaced with a CLIP retrieval module. Specifically, for each medical visual question, the ModCLIPs are employed to retrieve documents through both image-to-text and text-to-text retrieval. The two retrieval results are combined using Reciprocal Rank Fusion. We also ablate the DPO and SFT training stages of the MQG. The number of retrieved documents remains consistent. Our experiments demonstrate that MQG retrieves more relevant documents compared to standard CLIP methods. This improvement can be attributed to better alignment of MQG and each corpus’s characteristics. Furthermore, both the SFT and DPO training stages prove essential in developing MQG.

5.6 Alignment Effectiveness of HKPT

To evaluate the alignment effectiveness of HKPT, we introduce three additional metrics besides answer accuracy: Modality Disalignment (MD), Knowledge Usage Disalignment (KUD), and Knowledge Interference Disalignment (KID). MD corresponds to CMA in Section 4.3, KUD corresponds to KU, and KID corresponds to KR. MD measures

Models	OMVQA-Rad	OMVQA-Oph	Quilt-VQA
LLaVA-Med-7B	53.67	56.83	66.18
+ HeteroRAG	60.17	71.42	69.39
HuatuogPT-V-7B	72.08	81.83	66.18
+ HeteroRAG	78.17	84.50	71.43
Lingshu-7B	74.92	80.83	49.27
+ HeteroRAG	82.08	91.25	69.97

Table 6: Model performance when the HeteroRAG framework is applied to different Med-LVLMs.

the proportion that the Med-LVLM correctly answers with the irrelevant image among cases where it correctly answers with the original image. KUD measures the proportion that the Med-LVLM succeeds when any retrieval source (report, document, or report+document) is introduced among cases where it fails without retrieval. KID measures the proportion that the Med-LVLM fails when any retrieval source is introduced among cases where it succeeds without retrieval.

Figure 4 shows the average metrics on OMVQA-Rad, OMVQA-Oph, and Quilt-VQA. The “SFT” method refers to SFT using the training dataset with documents and reports added. The results demonstrate that HKPT improves overall accuracy compared to both the original and SFT models. Moreover, all three types of disalignment are significantly reduced by the HKPT method. We further conduct ablation studies on each type of preference pair in HKPT, including CMA, KU, and KR. The results confirm that each component effectively enhances the corresponding alignment capability as expected.

5.7 Compatibility Analysis

To analyze the compatibility of the HeteroRAG framework with different Med-LVLMs, we apply it to LLaVA-Med-7B and HuatuogPT-V-7B besides Lingshu-7B. Specifically, the ModCLIPs and MQG in HRM are kept unchanged, as they are universal across different downstream readers. The HKPT process is performed separately for each Med-LVLM. Results in Table 6 show that HeteroRAG brings consistent improvements over all Med-LVLMs. This indicates that HeteroRAG can be transferred to diverse Med-LVLMs.

6 Conclusion

This work addresses the critical challenges of effective retrieval and multi-aspect alignment for heterogeneous knowledge in the Medical MMRAG field. MedAtlas provides a rich, multi-source knowledge base for medical multimodal tasks. The HeteroRAG framework enables precise report retrieval and multi-corpus retrieval, followed by aligning heterogeneous retrieval results through Heterogeneous Knowledge Preference Tuning. Extensive experiments demonstrate that our framework achieves state-of-the-art performance across multiple medical VQA and report generation benchmarks. Our work paves the way for effectively integrating multi-source medical knowledge, advancing the reliability and applicability of Med-LVLMs in clinical scenarios.

References

- Bai, S.; Chen, K.; Liu, X.; Wang, J.; Ge, W.; Song, S.; Dang, K.; Wang, P.; Wang, S.; Tang, J.; et al. 2025. Qwen2. 5-v1 technical report. *arXiv preprint arXiv:2502.13923*.
- Banerjee, S.; and Lavie, A. 2005. METEOR: An Automatic Metric for MT Evaluation with Improved Correlation with Human Judgments. In Goldstein, J.; Lavie, A.; Lin, C.; and Voss, C. R., eds., *Proceedings of the Workshop on Intrinsic and Extrinsic Evaluation Measures for Machine Translation and/or Summarization@ACL 2005, Ann Arbor, Michigan, USA, June 29, 2005*, 65–72. Association for Computational Linguistics.
- Bodenreider, O. 2004. The Unified Medical Language System (UMLS): integrating biomedical terminology. *Nucleic Acids Res.*, 32(Database-Issue): 267–270.
- Chambon, P.; Delbrouck, J.-B.; Sounack, T.; Huang, S.-C.; Chen, Z.; Varma, M.; Truong, S. Q.; Chuong, C. T.; and Langlotz, C. P. 2024. Chexpert plus: Augmenting a large chest x-ray dataset with text radiology reports, patient demographics and additional image formats. *arXiv preprint arXiv:2405.19538*.
- Chen, J.; Ouyang, R.; Gao, A.; Chen, S.; Chen, G. H.; Wang, X.; Zhang, R.; Cai, Z.; Ji, K.; Yu, G.; Wan, X.; and Wang, B. 2024a. HuatuoGPT-Vision, Towards Injecting Medical Visual Knowledge into Multimodal LLMs at Scale. *CoRR*, abs/2406.19280.
- Chen, Z.; Hernández-Cano, A.; Romanou, A.; Bonnet, A.; Matoba, K.; Salvi, F.; Pagliardini, M.; Fan, S.; Köpf, A.; Mohtashami, A.; Sallinen, A.; Sakhaeirad, A.; Swamy, V.; Krawczuk, I.; Bayazit, D.; Marmet, A.; Montariol, S.; Hartley, M.; Jaggi, M.; and Bosselut, A. 2023. MEDITRON-70B: Scaling Medical Pretraining for Large Language Models. *CoRR*, abs/2311.16079.
- Chen, Z.; Liao, Y.; Jiang, S.; Wang, P.; Guo, Y.; Wang, Y.; and Wang, Y. 2025. Towards Omni-RAG: Comprehensive Retrieval-Augmented Generation for Large Language Models in Medical Applications. *arXiv preprint arXiv:2501.02460*.
- Chen, Z.; Wu, J.; Wang, W.; Su, W.; Chen, G.; Xing, S.; Zhong, M.; Zhang, Q.; Zhu, X.; Lu, L.; et al. 2024b. Internvl: Scaling up vision foundation models and aligning for generic visual-linguistic tasks. In *Proceedings of the IEEE/CVF Conference on Computer Vision and Pattern Recognition*, 24185–24198.
- Choi, K.; Yoon, B.; Kim, S.; and Park, J. 2025. Leveraging LLMs for Multimodal Retrieval-Augmented Radiology Report Generation via Key Phrase Extraction. *arXiv preprint arXiv:2504.07415*.
- Chu, Y.; Zhang, K.; Malon, C.; and Min, M. R. 2025. Reducing Hallucinations of Medical Multimodal Large Language Models with Visual Retrieval-Augmented Generation. *CoRR*, abs/2502.15040.
- Chuang, Y.; Xie, Y.; Luo, H.; Kim, Y.; Glass, J. R.; and He, P. 2024. DoLa: Decoding by Contrasting Layers Improves Factuality in Large Language Models. In *The Twelfth International Conference on Learning Representations, ICLR 2024, Vienna, Austria, May 7-11, 2024*. OpenReview.net.
- Comanici, G.; Bieber, E.; Schaekermann, M.; Pasupat, I.; Sachdeva, N.; Dhillon, I.; Blistein, M.; Ram, O.; Zhang, D.; Rosen, E.; et al. 2025. Gemini 2.5: Pushing the frontier with advanced reasoning, multimodality, long context, and next generation agentic capabilities. *arXiv preprint arXiv:2507.06261*.
- Decenciere, E.; Cazuguel, G.; Zhang, X.; Thibault, G.; Klein, J.-C.; Meyer, F.; Marcotegui, B.; Quéllec, G.; Lamard, M.; Danno, R.; et al. 2013. TeleOphta: Machine learning and image processing methods for teleophthalmology. *Irbm*, 34(2): 196–203.
- Demner-Fushman, D.; Kohli, M. D.; Rosenman, M. B.; Shooshan, S. E.; Rodriguez, L.; Antani, S.; Thoma, G. R.; and McDonald, C. J. 2015. Preparing a collection of radiology examinations for distribution and retrieval. *Journal of the American Medical Informatics Association*, 23(2): 304–310.
- Du, L.; Ho, A. T. S.; and Cong, R. 2020. Perceptual hashing for image authentication: A survey. *Signal Process. Image Commun.*, 81.
- Eslami, S.; Meinel, C.; and De Melo, G. 2023. PubMed-CLIP: How Much Does CLIP Benefit Visual Question Answering in the Medical Domain? In *Findings of the Association for Computational Linguistics: EACL 2023*, 1151–1163.
- Fan, R.-Z.; Wang, Z.; and Liu, P. 2025. MegaScience: Pushing the Frontiers of Post-Training Datasets for Science Reasoning. *arXiv:2507.16812*.
- Favero, A.; Zancato, L.; Trager, M.; Choudhary, S.; Perera, P.; Achille, A.; Swaminathan, A.; and Soatto, S. 2024. Multi-Modal Hallucination Control by Visual Information Grounding. In *IEEE/CVF Conference on Computer Vision and Pattern Recognition, CVPR 2024, Seattle, WA, USA, June 16-22, 2024*, 14303–14312. IEEE.
- Gamper, J.; and Rajpoot, N. 2021. Multiple instance captioning: Learning representations from histopathology textbooks and articles. In *Proceedings of the IEEE/CVF conference on computer vision and pattern recognition*, 16549–16559.
- Hamza, A.; Abdullah, A.; Ahn, Y. H.; Lee, S.; and Kim, S. T. 2025. LLaVA Needs More Knowledge: Retrieval Augmented Natural Language Generation with Knowledge Graph for Explaining Thoracic Pathologies. In Walsh, T.; Shah, J.; and Kolter, Z., eds., *AAAI-25, Sponsored by the Association for the Advancement of Artificial Intelligence, February 25 - March 4, 2025, Philadelphia, PA, USA*, 3311–3319. AAAI Press.
- He, S.; Nie, Y.; Chen, Z.; Cai, Z.; Wang, H.; Yang, S.; and Chen, H. 2024. MedDr: Diagnosis-Guided Bootstrapping for Large-Scale Medical Vision-Language Learning. *CoRR*, abs/2404.15127.
- He, X.; Zhang, Y.; Mou, L.; Xing, E. P.; and Xie, P. 2020. PathVQA: 30000+ Questions for Medical Visual Question Answering. *CoRR*, abs/2003.10286.
- Hu, E. J.; Shen, Y.; Wallis, P.; Allen-Zhu, Z.; Li, Y.; Wang, S.; Wang, L.; and Chen, W. 2022. LoRA: Low-Rank Adaptation of Large Language Models. In *The Tenth International*

- Conference on Learning Representations, ICLR 2022, Virtual Event, April 25-29, 2022*. OpenReview.net.
- Hu, Y.; Li, T.; Lu, Q.; Shao, W.; He, J.; Qiao, Y.; and Luo, P. 2024. OmniMedVQA: A New Large-Scale Comprehensive Evaluation Benchmark for Medical LVLm. In *IEEE/CVF Conference on Computer Vision and Pattern Recognition, CVPR 2024, Seattle, WA, USA, June 16-22, 2024*, 22170–22183. IEEE.
- Huang, J.-H.; Yang, C.-H. H.; Liu, F.; Tian, M.; Liu, Y.-C.; Wu, T.-W.; Lin, I.; Wang, K.; Morikawa, H.; Chang, H.; et al. 2021. Deepopt: medical report generation for retinal images via deep models and visual explanation. In *Proceedings of the IEEE/CVF winter conference on applications of computer vision*, 2442–2452.
- Ikezogwo, W.; Seyfioglu, S.; Ghezloo, F.; Geva, D.; Sheikh Mohammed, F.; Anand, P. K.; Krishna, R.; and Shapiro, L. 2023. Quilt-1m: One million image-text pairs for histopathology. *Advances in neural information processing systems*, 36: 37995–38017.
- Jin, D.; Pan, E.; Oufattole, N.; Weng, W.-H.; Fang, H.; and Szolovits, P. 2020. What Disease does this Patient Have? A Large-scale Open Domain Question Answering Dataset from Medical Exams. *arXiv preprint arXiv:2009.13081*.
- Jin, Q.; Kim, W.; Chen, Q.; Comeau, D. C.; Yeganova, L.; Wilbur, W. J.; and Lu, Z. 2023. MedCPT: Contrastive pre-trained transformers with large-scale pubmed search logs for zero-shot biomedical information retrieval. *Bioinformatics*, 39(11): btad651.
- Johnson, A. E.; Pollard, T. J.; Greenbaum, N. R.; Lungren, M. P.; Deng, C.-y.; Peng, Y.; Lu, Z.; Mark, R. G.; Berkowitz, S. J.; and Horng, S. 2019. MIMIC-CXR-JPG, a large publicly available database of labeled chest radiographs. *arXiv preprint arXiv:1901.07042*.
- Lau, J. J.; Gayen, S.; Ben Abacha, A.; and Demner-Fushman, D. 2018. A dataset of clinically generated visual questions and answers about radiology images. *Scientific data*, 5(1): 1–10.
- Leng, S.; Zhang, H.; Chen, G.; Li, X.; Lu, S.; Miao, C.; and Bing, L. 2024. Mitigating Object Hallucinations in Large Vision-Language Models through Visual Contrastive Decoding. In *IEEE/CVF Conference on Computer Vision and Pattern Recognition, CVPR 2024, Seattle, WA, USA, June 16-22, 2024*, 13872–13882. IEEE.
- Li, C.; Wong, C.; Zhang, S.; Usuyama, N.; Liu, H.; Yang, J.; Naumann, T.; Poon, H.; and Gao, J. 2023. LLaVA-Med: Training a Large Language-and-Vision Assistant for Biomedicine in One Day. In Oh, A.; Naumann, T.; Globerson, A.; Saenko, K.; Hardt, M.; and Levine, S., eds., *Advances in Neural Information Processing Systems 36: Annual Conference on Neural Information Processing Systems 2023, NeurIPS 2023, New Orleans, LA, USA, December 10 - 16, 2023*.
- Li, J.; Su, T.; Zhao, B.; Lv, F.; Wang, Q.; Navab, N.; Hu, Y.; and Jiang, Z. 2024. Ultrasound report generation with cross-modality feature alignment via unsupervised guidance. *IEEE Transactions on Medical Imaging*.
- Li, M.; Cai, W.; Liu, R.; Weng, Y.; Zhao, X.; Wang, C.; Chen, X.; Liu, Z.; Pan, C.; Li, M.; et al. 2021. FFA-IR: Towards an explainable and reliable medical report generation benchmark. In *Thirty-fifth conference on neural information processing systems datasets and benchmarks track (round 2)*.
- Lin, C.-Y. 2004. ROUGE: A Package for Automatic Evaluation of Summaries. In *Text Summarization Branches Out*, 74–81. Barcelona, Spain: Association for Computational Linguistics.
- Lin, T.; Zhang, W.; Li, S.; Yuan, Y.; Yu, B.; Li, H.; He, W.; Jiang, H.; Li, M.; Song, X.; Tang, S.; Xiao, J.; Lin, H.; Zhuang, Y.; and Ooi, B. C. 2025. HealthGPT: A Medical Large Vision-Language Model for Unifying Comprehension and Generation via Heterogeneous Knowledge Adaptation. *CoRR*, abs/2502.09838.
- Lin, W.; Zhao, Z.; Zhang, X.; Wu, C.; Zhang, Y.; Wang, Y.; and Xie, W. 2023. PMC-CLIP: Contrastive Language-Image Pre-training Using Biomedical Documents. In *International Conference on Medical Image Computing and Computer-Assisted Intervention*, 525–536.
- Liu, B.; Zhan, L.; Xu, L.; Ma, L.; Yang, Y.; and Wu, X. 2021. Slake: A Semantically-Labeled Knowledge-Enhanced Dataset For Medical Visual Question Answering. In *18th IEEE International Symposium on Biomedical Imaging, ISBI 2021, Nice, France, April 13-16, 2021*, 1650–1654. IEEE.
- Luo, Y.; Shi, M.; Khan, M. O.; Afzal, M. M.; Huang, H.; Yuan, S.; Tian, Y.; Song, L.; Kouhana, A.; Elze, T.; et al. 2024. FairCLIP: Harnessing fairness in vision-language learning. In *Proceedings of the IEEE/CVF Conference on Computer Vision and Pattern Recognition*, 12289–12301.
- NCBI. 2025. PubMed Baseline Data. <https://ftp.ncbi.nlm.nih.gov/pubmed/baseline/>.
- Papineni, K.; Roukos, S.; Ward, T.; and Zhu, W. 2002. Bleu: a Method for Automatic Evaluation of Machine Translation. In *Proceedings of the 40th Annual Meeting of the Association for Computational Linguistics, July 6-12, 2002, Philadelphia, PA, USA*, 311–318. ACL.
- Porwal, P.; Pachade, S.; Kamble, R.; Kokare, M.; Deshmukh, G.; Sahasrabudde, V.; and Mériaudeau, F. 2018. Indian Diabetic Retinopathy Image Dataset (IDRiD): A Database for Diabetic Retinopathy Screening Research. *Data*, 3(3): 25.
- Radford, A.; Kim, J. W.; Hallacy, C.; Ramesh, A.; Goh, G.; Agarwal, S.; Sastry, G.; Askell, A.; Mishkin, P.; Clark, J.; Krueger, G.; and Sutskever, I. 2021. Learning Transferable Visual Models From Natural Language Supervision. In Meila, M.; and Zhang, T., eds., *Proceedings of the 38th International Conference on Machine Learning, ICML 2021, 18-24 July 2021, Virtual Event*, volume 139 of *Proceedings of Machine Learning Research*, 8748–8763. PMLR.
- Ranjit, M. P.; Ganapathy, G.; Manuel, R.; and Ganu, T. 2023. Retrieval Augmented Chest X-Ray Report Generation using OpenAI GPT models. In Deshpande, K.; Fiterau, M.; Joshi, S.; Lipton, Z. C.; Ranganath, R.; Urteaga, I.; and Yeung, S., eds., *Machine Learning for Healthcare Conference*,

- MLHC 2023, 11-12 August 2023, New York, USA, volume 219 of *Proceedings of Machine Learning Research*, 650–666. PMLR.
- Rückert, J.; Bloch, L.; Brüngel, R.; Idrissi-Yaghir, A.; Schäfer, H.; Schmidt, C. S.; Koitka, S.; Pelka, O.; Abacha, A. B.; G. Seco de Herrera, A.; et al. 2024. ROCov2: Radiology objects in context version 2, an updated multimodal image dataset. *Scientific Data*, 11(1): 688.
- Sellergren, A.; Kazemzadeh, S.; Jaroensri, T.; Kiraly, A.; Traverse, M.; Kohlberger, T.; Xu, S.; Jamil, F.; Hughes, C.; Lau, C.; et al. 2025. MedGemma Technical Report. *arXiv preprint arXiv:2507.05201*.
- Seyfioglu, M. S.; Ikezogwo, W. O.; Ghezloo, F.; Krishna, R.; and Shapiro, L. G. 2024. Quilt-LLaVA: Visual Instruction Tuning by Extracting Localized Narratives from Open-Source Histopathology Videos. In *IEEE/CVF Conference on Computer Vision and Pattern Recognition, CVPR 2024, Seattle, WA, USA, June 16-22, 2024*, 13183–13192. IEEE.
- Shaaban, M. A.; Saleem, T. J.; Papineni, V. R.; and Yaqub, M. 2025. MOTOR: Multimodal Optimal Transport via Grounded Retrieval in Medical Visual Question Answering. *arXiv preprint arXiv:2506.22900*.
- StatPearls. 2024. StatPearls. <https://www.ncbi.nlm.nih.gov/books/NBK430685/>.
- Sun, L.; Zhao, J. J.; Han, W.; and Xiong, C. 2025. Fact-Aware Multimodal Retrieval Augmentation for Accurate Medical Radiology Report Generation. In *Proceedings of the 2025 Conference of the Nations of the Americas Chapter of the Association for Computational Linguistics: Human Language Technologies (Volume 1: Long Papers)*, 643–655.
- Sun, Y.; Wu, H.; Zhu, C.; Zheng, S.; Chen, Q.; Zhang, K.; Zhang, Y.; Wan, D.; Lan, X.; Zheng, M.; Li, J.; Lyu, X.; Lin, T.; and Yang, L. 2024a. PathMMU: A Massive Multimodal Expert-Level Benchmark for Understanding and Reasoning in Pathology. In Leonardis, A.; Ricci, E.; Roth, S.; Rusakovsky, O.; Sattler, T.; and Varol, G., eds., *Computer Vision - ECCV 2024 - 18th European Conference, Milan, Italy, September 29-October 4, 2024, Proceedings, Part LXII*, volume 15120 of *Lecture Notes in Computer Science*, 56–73. Springer.
- Sun, Y.; Zhu, C.; Zheng, S.; Zhang, K.; Sun, L.; Shui, Z.; Zhang, Y.; Li, H.; and Yang, L. 2024b. Pathasst: A generative foundation ai assistant towards artificial general intelligence of pathology. In *Proceedings of the AAAI Conference on Artificial Intelligence*, volume 38, 5034–5042.
- Sutskever, I.; Vinyals, O.; and Le, Q. V. 2014. Sequence to Sequence Learning with Neural Networks. In Ghahramani, Z.; Welling, M.; Cortes, C.; Lawrence, N. D.; and Weinberger, K. Q., eds., *Advances in Neural Information Processing Systems 27: Annual Conference on Neural Information Processing Systems 2014, December 8-13 2014, Montreal, Quebec, Canada*, 3104–3112.
- Tascon-Morales, S.; Márquez-Neila, P.; and Sznitman, R. 2022. Consistency-Preserving Visual Question Answering in Medical Imaging. In Wang, L.; Dou, Q.; Fletcher, P. T.; Speidel, S.; and Li, S., eds., *Medical Image Computing and Computer Assisted Intervention - MICCAI 2022 - 25th International Conference, Singapore, September 18-22, 2022, Proceedings, Part VIII*, volume 13438 of *Lecture Notes in Computer Science*, 386–395. Springer.
- Tsuneki, M.; and Kanavati, F. 2022. Inference of captions from histopathological patches. In *International Conference on Medical Imaging with Deep Learning*, 1235–1250. PMLR.
- Wang, J.; Ashraf, T.; Han, Z.; Laaksonen, J.; and Anwer, R. M. 2025. MIRA: A Novel Framework for Fusing Modalities in Medical RAG. *arXiv preprint arXiv:2507.07902*.
- Wikimedia. 2023. Wikimedia Wikipedia. <https://huggingface.co/datasets/wikimedia/wikipedia>.
- Woo, S.; Kim, D.; Jang, J.; Choi, Y.; and Kim, C. 2024. Don't Miss the Forest for the Trees: Attentional Vision Calibration for Large Vision Language Models. *CoRR*, abs/2405.17820.
- Wu, C.; Lin, W.; Zhang, X.; Zhang, Y.; Xie, W.; and Wang, Y. 2024a. PMC-LLaMA: toward building open-source language models for medicine. *J. Am. Medical Informatics Assoc.*, 31(9): 1833–1843.
- Wu, R.; Zhang, C.; Zhang, J.; Zhou, Y.; Zhou, T.; and Fu, H. 2024b. MM-retinal: Knowledge-enhanced foundational pre-training with fundus image-text expertise. In *International Conference on Medical Image Computing and Computer-Assisted Intervention*, 722–732. Springer.
- Wu, Y.; Lu, Y.; Zhou, Y.; Ding, Y.; Liu, J.; and Ruan, T. 2025. MKGF: A multi-modal knowledge graph based RAG framework to enhance LVLMS for Medical visual question answering. *Neurocomputing*, 635: 129999.
- Xia, P.; Zhu, K.; Li, H.; Wang, T.; Shi, W.; Wang, S.; Zhang, L.; Zou, J.; and Yao, H. 2025. MMed-RAG: Versatile Multimodal RAG System for Medical Vision Language Models. In *The Thirteenth International Conference on Learning Representations*.
- Xia, P.; Zhu, K.; Li, H.; Zhu, H.; Li, Y.; Li, G.; Zhang, L.; and Yao, H. 2024. RULE: Reliable Multimodal RAG for Factuality in Medical Vision Language Models. In *Proceedings of the 2024 Conference on Empirical Methods in Natural Language Processing*, 1081–1093.
- Xiong, G.; Jin, Q.; Lu, Z.; and Zhang, A. 2024. Benchmarking Retrieval-Augmented Generation for Medicine. In Ku, L.; Martins, A.; and Srikumar, V., eds., *Findings of the Association for Computational Linguistics, ACL 2024, Bangkok, Thailand and virtual meeting, August 11-16, 2024*, 6233–6251. Association for Computational Linguistics.
- Xu, W.; Chan, H. P.; Li, L.; Aljunied, M.; Yuan, R.; Wang, J.; Xiao, C.; Chen, G.; Liu, C.; Li, Z.; et al. 2025. Lingshu: A Generalist Foundation Model for Unified Multimodal Medical Understanding and Reasoning. *arXiv preprint arXiv:2506.07044*.
- Yang, R.; Liu, H.; Marrese-Taylor, E.; Zeng, Q.; Ke, Y.; Li, W.; Cheng, L.; Chen, Q.; Caverlee, J.; Matsuo, Y.; and Li, I. 2024. KG-Rank: Enhancing Large Language Models for Medical QA with Knowledge Graphs and Ranking Techniques. In Demner-Fushman, D.; Ananiadou, S.; Miwa,

M.; Roberts, K.; and Tsujii, J., eds., *Proceedings of the 23rd Workshop on Biomedical Natural Language Processing, BioNLP@ACL 2024, Bangkok, Thailand, August 16, 2024*, 155–166. Association for Computational Linguistics.

Zhang, S.; Xu, Y.; Usuyama, N.; Xu, H.; Bagga, J.; Tinn, R.; Preston, S.; Rao, R.; Wei, M.; Valluri, N.; et al. 2023. BiomedCLIP: a multimodal biomedical foundation model pretrained from fifteen million scientific image-text pairs. *arXiv preprint arXiv:2303.00915*.

Zhao, W.; Wu, C.; Zhang, X.; Zhang, Y.; Wang, Y.; and Xie, W. 2024a. RaTEScore: A Metric for Radiology Report Generation. In *Proceedings of the 2024 Conference on Empirical Methods in Natural Language Processing*, 15004–15019.

Zhao, Z.; Wang, S.; Gu, J.; Zhu, Y.; Mei, L.; Zhuang, Z.; Cui, Z.; Wang, Q.; and Shen, D. 2024b. ChatCAD+: Toward a universal and reliable interactive CAD using LLMs. *IEEE Transactions on Medical Imaging*, 43(11): 3755–3766.

A Additional Analysis

A.1 Qualitative Analysis

We provide three case studies in Figure 5. For the first case, HeteroRAG outperforms Lingshu-7B by effectively leveraging external knowledge for reasoning. It utilizes the retrieved document’s description of “typical MRI signal characteristics of fat-containing tumors” to recognize imaging features indicative of fat content in the lesion, thereby supporting the correct answer. Lingshu-7B lacks access to external knowledge and provides an incorrect response.

For the second case, HeteroRAG outperforms Lingshu-7B by effectively leveraging retrieved reports. It refers to key phrases: “Low lung volumes are present,” and the impression: “Low lung volumes with probable bibasilar atelectasis. No evidence of congestive heart failure.” The similar reports enable clinically accurate, well-supported conclusions for HeteroRAG.

For the third case, HeteroRAG effectively leveraged both retrieved contents. Retrieved reports explicitly state, “intravascular pyogenic granulomas show a lobular growth pattern of well-formed capillaries,” where “lobular growth pattern” directly corresponds to the “architectural pattern” in the question. Additionally, the retrieved documents include a research entry mentioning “infiltrating lobular carcinoma,” further complementing information for lobular, which is a well-established histopathological architectural pattern. HeteroRAG integrated this multi-source knowledge to confirm “lobular” as the correct answer, highlighting HeteroRAG’s advantage in factuality and reliability.

A.2 Impact of Retrieved Report Images

Methods	OMVQA-Rad	OMVQA-Oph	Quilt-VQA
Original	74.92	80.83	49.27
MMed-RAG	79.50	88.17	67.06
+ Report Images	76.42	86.83	63.56
HeteroRAG	82.08	91.25	69.97
+ Report Images	80.08	89.50	72.59

Table 7: Model performance when the retrieved report images are incorporated.

We further explore the integration of retrieved report images into Med-LVLMs inspired by V-RAG (Chu et al. 2025). Specifically, we incorporate retrieved report images in constructing the preference pairs and training models. Results in Table 7 indicate that adding report images does not improve model performance and even leads to degradation on most datasets. We attribute this to visual information in report images that is redundant with the report text, potentially hindering the model’s ability to align and integrate external knowledge. Therefore, we do not include retrieved report images in our main methods.

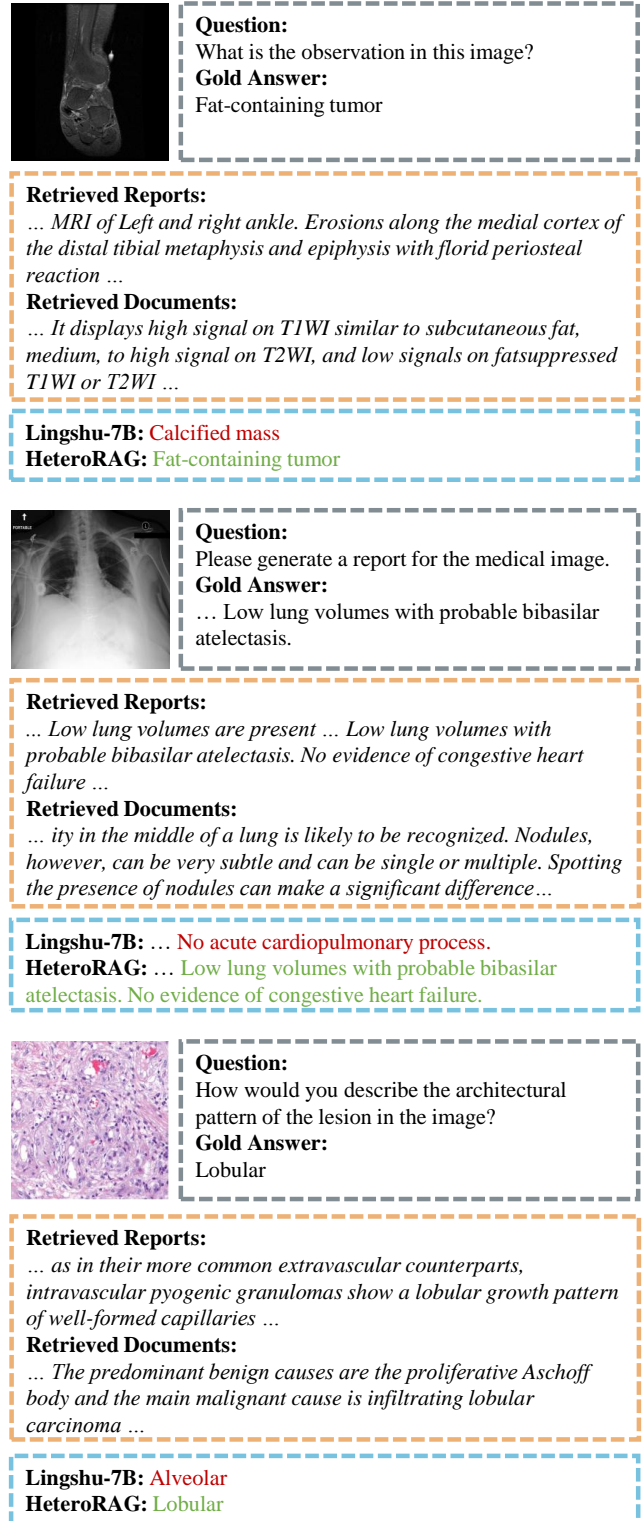


Figure 5: Qualitative analyses for the superiority of HeteroRAG.

Source	Modality	# Pairs	# Total
IU-Xray		495	
PLA		14.7k	
CheXpert-Plus	Rad.	187.6k	1.1M
MIMIC-CXR		209.6k	
ROCOv2		79.8k	
PMC-OA-Rad		612.2k	
Harvard-FairVLMed		5.0k	
DeepEyeNet		2.9k	
FFA-IR	Oph.	44.7k	112.0k
MM-Retinal		4.4k	
PMC-OA-Oph		55.1k	
ARCH		6.8k	
PathCap		221.3k	
PatchGastric	Pat.	262.8k	1.5M
Quilt-1M		433.9k	
PMC-OA-Pat		589.3k	

Table 8: Statistics of multimodal report knowledge base in MedAtlas.

Source	Corpus	# Chunks	# Total
PubMed	Research	51.2M	51.2M
Wikipedia	Wiki	29.7M	29.7M
PMC-LLaMA		13.7M	
MedQA	Book	125.8k	14.1M
StatPearls		322.7k	
Meditron	Guideline	657.9k	657.9k
-	-	# Terms	# Relations
UMLS	Graph	1.7M	2.9M

Table 9: Statistics of textual corpora in MedAtlas.

B Additional Details

B.1 MedAtlas Details

The statistics of the multimodal report knowledge base and textual corpora in MedAtlas are shown in Table 8 and Table 9, respectively. For the multimodal report knowledge base, its radiology subset includes IU-Xray (Demner-Fushman et al. 2015), PLA (Li et al. 2024), CheXpert-Plus (Chambon et al. 2024), MIMIC-CXR (Johnson et al. 2019), ROCov2 (Rückert et al. 2024), and PMC-OA-Rad (Lin et al. 2023). The ophthalmology subset includes Harvard-FairVLMed (Luo et al. 2024), DeepEyeNet (Huang et al. 2021), FFA-IR (Li et al. 2021), MM-Retinal (Wu et al. 2024b), and PMC-OA-Oph (Lin et al. 2023). The pathology subset includes ARCH (Gamper and Rajpoot 2021), PathCap (Sun et al. 2024b), PatchGastric (Tsuneki and Kanavati 2022), Quilt-1M (Ikezogwo et al. 2023), and PMC-OA-Pat (Lin et al. 2023).

The textual knowledge base of MedAtlas encompasses a diverse collection of biomedical and general-domain cor-

pora. The Research corpus includes PubMed Annual Baseline (NCBI 2025), a comprehensive collection of biomedical literature. The Wiki corpus includes Wikipedia (Wikipedia 2023), providing broad-domain textual knowledge. The Book corpus comprises PMC-LLaMA Books (Wu et al. 2024a), MedQA Textbooks (Jin et al. 2020), and StatPearls (StatPearls 2024), offering in-depth medical knowledge from authoritative sources. The Guideline corpus includes Meditron Guidelines (Chen et al. 2023), which contains curated clinical practice guidelines. The Graph corpus is from UMLS Metathesaurus (Bodenreider 2004), a comprehensive semantic network that integrates concepts and relationships from multiple biomedical vocabularies.

B.2 Dataset Details

The datasets used in our work include medical VQA datasets and medical report generation datasets. The VQA datasets are introduced as follows:

- **OMVQA-Rad** (Hu et al. 2024) is the radiology subset of the OmniMedVQA dataset, which aggregates data from multiple medical classification datasets and converts them into a VQA format. We employ the open-access subset. We randomly select 4,200 samples for the training set and 1,200 samples for the test set.
- **VQA-RAD** (Lau et al. 2018) is the first manually curated VQA dataset in radiology, where clinical questions were naturally formulated by medical professionals based on radiological images, along with reference answers. We employ the closed-ended subset. We use the official training split of size 1,027 and the official test split of size 272.
- **SLAKE** (Liu et al. 2021) is a large bilingual medical VQA dataset featuring comprehensive semantic annotations by experienced physicians, accompanied by a structured medical knowledge base. We employ the English closed-ended subset. We use the official training split of size 1,943 and the official test split of size 416.
- **OMVQA-Oph** (Hu et al. 2024) is the ophthalmology subset derived from the OmniMedVQA dataset. We employ the open-access subset. We randomly select 4,200 samples for the training set and 1,200 samples for the test set.
- **DME-VQA** (Tascon-Morales, Márquez-Neila, and Sznitman 2022) is built upon two public retinal image datasets, IDRiD (Porwal et al. 2018) and e-Ophta (Decenciere et al. 2013), containing questions related to diabetic macular edema (DME) and other eye conditions. The contours of the original image masks are extracted and rendered as red outlines on the original images to form the question images for each sample. We randomly select 5,000 samples from the official training split for the training set and use the official test split of size 1,311.
- **Quilt-VQA** (Seyfioglu et al. 2024) is an organic evaluation dataset created by extracting real-world medical questions and answers from QUILT educational videos. We employ the closed-ended subset. We use the official test split of size 343.

- **PathMMU** (Sun et al. 2024a) is a high-quality, diverse pathology VQA dataset designed to assess the reasoning and understanding capabilities of large multimodal models in pathology. We employ its PathCLS and Atlas subsets, as they are not included in the pretraining data of Lingshu-7B to the best of our knowledge. Then we randomly select 2,095 samples for the training set and 598 samples for the test set.
- **PathVQA** (He et al. 2020) is the first VQA dataset in pathology, constructed using a semi-automated pipeline that extracts question-answer pairs from pathology textbooks and digital libraries. We employ the closed-ended subset. We randomly select 5,000 samples from the official training split for the training set and use the official test split of size 3,391.

The medical report generation datasets are described as follows:

- **MIMIC-CXR** (Johnson et al. 2019) is a large, publicly available collection of chest radiographs in DICOM format, paired with free-text radiology reports from studies conducted at the Beth Israel Deaconess Medical Center in Boston, MA. We exclude the samples that do not contain findings or impressions. We randomly select 5,000 samples from the official training split for the training set and use the official test split of size 1,624.
- **IU-Xray** (Demner-Fushman et al. 2015) consists of chest X-ray images linked to their corresponding clinical diagnostic reports. We exclude the samples that do not contain findings or impressions. We use the official training split of size 2,445 and the official test split of size 296.
- **Harvard-FairVLMed** (Luo et al. 2024) includes patient records with SLO fundus images and clinical notes for glaucoma diagnosis. We randomly select 3,500 samples from the official training split for the training set and 1,000 samples from the official test split for the test set.
- **DeepEyeNet** (Huang et al. 2021) is a large-scale retinal image dataset containing two modalities: grayscale fluorescein angiography (FA) and color fundus photographs (CFP), supporting various ophthalmic analysis tasks. We randomly select 5,000 samples from the official training split for the training set and use the official test split of size 3,140.

B.3 Baseline Details

Decoding-based methods aiming to improve factuality are described as follows:

- **Original** uses greedy decoding, which selects the token with the highest probability at each generation step, favoring locally optimal choices without considering long-term sequence quality.
- **Beam Search** (Sutskever, Vinyals, and Le 2014) improves upon greedy decoding by keeping track of multiple partial sequences (beams) at each step, exploring a wider range of potential outputs and often yielding more coherent and accurate generations.
- **DoLa** (Chuang et al. 2024) leverages the discrepancy between early and later layer representations in the model

by comparing their projected logits onto the vocabulary space, guiding generation toward more accurate and contextually appropriate tokens.

- **VCD** (Leng et al. 2024) introduces a training-free decoding strategy that compares outputs from original and perturbed visual inputs, helping to mitigate model reliance on statistical bias and unimodal priors.
- **AVISC** (Woo et al. 2024) is a test-time decoding method that enhances visual understanding by dynamically recalibrating attention during token generation, specifically reducing over-attention to image tokens that lack task-relevant content.
- **M3ID** (Favero et al. 2024) strengthens the impact of the reference image during generation by amplifying tokens that have higher mutual information with the visual input.

Medical report-retrieval methods are described as follows:

- **MedDr** (He et al. 2024) employs a retrieval-augmented medical diagnosis strategy in the inference process to improve the factuality of the model’s responses.
- **FactMM-RAG** (Sun et al. 2025) feeds the multimodal question together with the retrieved report to the Med-LVLM, which is fine-tuned using standard SFT to better incorporate external reports.
- **RULE** (Xia et al. 2024) constructs a preference dataset focusing on cases where over-reliance on retrieved reports causes errors, aiming to balance the use of internal knowledge and external context.
- **MMed-RAG** (Xia et al. 2025) extends RULE (Xia et al. 2024) by introducing cross-modality alignment to ensure image utilization and proposing overall alignment to better incorporate external reports.

Medical document-retrieval methods are described as follows:

- **MKGF** (Wu et al. 2025) uses a multimodal retriever to fetch knowledge graphs and supplement knowledge for LVLMs. We reproduce it using ModCLIP for image-to-text and text-to-text retrieval to retrieve text corpora, combining results via Reciprocal Rank Fusion.
- **K-LLaVA** (Hamza et al. 2025) retrieves relevant KG triplets using a CLIP model and fine-tunes the LVLM to incorporate the knowledge. We also use ModCLIP for retrieval in this method.

A concurrent work that retrieves both reports and documents is described as follows:

- **MIRA** (Wang et al. 2025) is a concurrent method that retrieves both medical reports and documents. To reproduce it, we use the input image to retrieve similar clinical cases and employ a zero-shot query-rewriting module (Lingshu-7B) for corpus retrieval. Then the downstream reader is fine-tuned, whose training data includes a chain-of-thought to guide the reader in analyzing the external knowledge.

We also introduce widely used Med-LVLMs, which are described as follows:

- **LLaVA-Med-7B** (Li et al. 2023) first aligns biomedical terminology using figure-caption pairs from scientific literature, then enhances conversational understanding through GPT-4-generated instruction-following data, simulating the way non-experts gradually acquire medical knowledge through.
- **MedGemma-4B** (Sellergren et al. 2025) is developed by Google and exhibits strong medical image and text understanding capabilities, significantly outperforming other generative models of similar size and approaching the performance of specialized task-specific models.
- **HuatuoGPT-V-34B** (Chen et al. 2024a) is trained on PubMedVision, a large-scale dataset of 1.3 million medical VQA samples constructed by refining image-text pairs from PubMed with the help of MLLMs (e.g., GPT-4V), showing superior performance in medical multimodal scenarios.
- **HealthGPT-32B** (Lin et al. 2025) integrates medical visual comprehension and generation into a unified autoregressive framework, progressively adapting heterogeneous multimodal knowledge to a pre-trained LLM through a bootstrapping approach.
- **Lingshu-32B** (Xu et al. 2025) is developed based on a carefully curated multimodal dataset enriched with comprehensive medical knowledge, undergoing multi-stage training to progressively embed domain expertise and improve task-solving abilities, consistently outperforming existing open-source models in most medical multimodal benchmarks.

B.4 Implementation Details

For the training of ModCLIPs, they are initialized from BiomedCLIP (Zhang et al. 2023). The learning rate is set to $2e-4$, and the batch size is set to 512. The number of training epochs of radiology, ophthalmology, and pathology ModCLIP is set to 10, 100, and 10, respectively, for the different sizes of modality image-text pairs.

For the training of MQG, the Med-LVLM is initialized from Lingshu-7B (Xu et al. 2025). We use LoRA (Hu et al. 2022) for efficient fine-tuning. For the SFT process, its learning rate is set to $2e-4$, the batch size is set to 64, and the number of epochs is 3. For the DPO process, its learning rate is set to $2e-5$, the batch size is set to 64, and the number of epochs is set to 3.

For the training of HKPT, the Med-LVLM is initialized from Lingshu-7B. We also use LoRA (Hu et al. 2022) for efficient fine-tuning. Its learning rate is set to $2e-5$, the batch size is set to 64, and the number of epochs is set to 4.

In our experiments, we use the development set, which has no overlap with the training and test sets, to tune the hyperparameters. The temperature of generation is set to 0 to ensure reproducibility. Huggingface Trainer is adopted as the training framework for Med-LVLMs.

C Prompt List

Prompt C.1: VQA with Retrieved Reports and Documents

{question_image}

Retrieved Contents:
{text_doc}

Reference Reports:
{mm_doc}

{question_text}

Please answer the question based on the Retrieved Contents. It should be noted that the diagnostic information in the Reference Reports cannot be directly used as the basis for diagnosis, but should only be used for reference and comparison.

Answer with the option's letter from the given choices directly.

Prompt C.2: Report Generation with Retrieved Reports and Documents

{question_image}

Retrieved Contents:
{text_doc}

Reference Reports:
{mm_doc}

Please answer the question based on the Retrieved Contents. It should be noted that the diagnostic information in the Reference Reports cannot be directly used as the basis for diagnosis, but should only be used for reference and comparison.

(For radiology) You are a helpful assistant. Please generate a report for the given image, including both findings and impressions. Return the report in the following format: Findings: {} Impression: {}.
(For ophthalmology) You are a helpful assistant. Please generate a short report for the given image in 100 words. Please only include the content of the report in your response.

Prompt C.3: Query Exploration by the Expert Med-LVLM

{question_image}

Question (based on the image)
{question_text}

Corpus Description

research: The corpus provides access to advanced biomedical research, facilitating access to specialized knowledge and resources.

wiki: The corpus provides access to general knowledge across a wide range of topics.

book: The corpus provides access to medical knowledge resource including various educational resources and textbooks.

guideline: The corpus provides access to clinical guidelines from leading health organizations.

graph: The corpus provides a structured knowledge graph that connects medical definitions and related terms.

Query Format

<research>{query0} ; {query1} ; ... (Use ; to separate the queries)</research>

<wiki>{query0} ; {query1} ; ... (Use ; to separate the queries)</wiki>

<book>{query0} ; {query1} ; ... (Use ; to separate the queries)</book>

<guideline>{query0} ; {query1} ; ... (Use ; to separate the queries)</guideline>

<graph>{query_term0} , {query_relation0} ; {query_term1} , {query_relation1} ; ... (Use ; to separate the queries. Each query should use , to separate the {query_term} and {query_relation})</graph>

To answer the question labeled as # Question, please construct appropriate queries to get the information you need.

1. Each corpus in # Corpus Description must have search queries constructed.
2. Please give the search queries following the format in # Query Format. Each corpus should have 6 queries, separated by ','.
3. The queries generated for each corpus should exhibit diversity and be closely aligned with the specific information needs and characteristics of that corpus.

Prompt C.4: Query Judging through Retrieved Documents by the Expert Med-LVLM

{question_image}

Question (based on the image)

{question_text}

Gold Answer

{gold}

Documents

{documents}

You are a professional medical expert. Please judge whether the information in the # Documents supports the # Gold Answer as a response to the # Question. Please judge whether # Documents supports the # Gold Answer in response to the # Question, rather than evaluating if the # Question's answer is the # Gold Answer. Please first think step-by-step and then show your judgement using the format <answer>yes/no</answer> at the end of your response. Please keep your entire response simple and complete, up to 100 words.

Prompt C.5: Query Generation by the Multi-corpora Query Generator

{question_image}

Question (based on the image)

{question_text}

Corpus Description

research: The corpus provides access to advanced biomedical research, facilitating access to specialized knowledge and resources.

wiki: The corpus provides access to general knowledge across a wide range of topics.

book: The corpus provides access to medical knowledge resource including various educational resources and textbooks.

guideline: The corpus provides access to clinical guidelines from leading health organizations.

graph: The corpus provides a structured knowledge graph that connects medical definitions and related terms.

Query Format

<research>{query}</research>

<wiki>{query}</wiki>

<book>{query}</book>

<guideline>{query}</guideline>

<graph>{query_term} , {query_relation} (Each query should use , to separate the {query_term} and {query_relation})</graph>

To answer the question labeled as # Question, please construct appropriate queries to get the information you need.

1. Please give the search queries following the format in # Query Format. For each corpus, if you think no information retrieval is needed, simply output an empty tag for that corpus, for example: <book></book>.
2. The queries generated for each corpus should be closely aligned with the specific information needs and characteristics of that corpus.